Quaternary Science Reviews 171 (2017) 154–165

Contents lists available at ScienceDirect

Quaternary Science Reviews

journal homepage: www.elsevier.com/locate/quascirev

Depositional evolution of the Lower Khuzestan plain (SW Iran) since the end of the Late Pleistocene

Frieda Bogemans [a, *], Rindert Janssens [a], Cecile Baeteman [a, b]

[a] Quaternary Environments & Humans, Royal Belgian Institute of Natural Sciences, Jennerstraat 13, B-1000 Brussels, Belgium
[b] Vrije Universiteit Brussel (VUB), MEMC, Pleinlaan 2, 1050 Brussel, Belgium

ARTICLE INFO

Article history:
Received 10 February 2017
Received in revised form
4 July 2017
Accepted 13 July 2017

Keywords:
Persian Gulf
Mesopotamia
Holocene
Mud-dominated river
Estuary
Evaporites
Climate change
Sea-level rise

ABSTRACT

A detailed sedimentological investigation of sixty-six cores supported by radiocarbon age determination enabled the reconstruction of the depositional environmental evolution since the end of the Late Pleistocene in the Iranian part of the Mesopotamian plain. Both fluvial and estuarine environments have been identified on the basis of the sediment characteristics and their between-core stratigraphic correlations. At the end of the Late Pleistocene the fluvial behaviour allowed only the deposition of sand. Prior to 12400–12040 yr cal BP the palaeohydraulics changed by which heterolithic fluvial facies were deposited. Shortly after 12400 - 12040 yr cal BP an erosional phase caused the incision of depressions most probably because of a climate change to further arid conditions. In the early Holocene, mud-dominated river systems filled the depressions; a situation that lasted at least until 7900 - 7700 yr cal BP. After this period tides invaded via the active channels in the downstream part of the area, which turned into an estuarine environment for a period of about 2000–2500 years. Tidal influence diminished and stopped around 5000 yr cal BP because of progradation. Fluvial processes dominated again the sedimentary environment in the study area, except at the southern margin of it where tides controlled, although very locally, the environment.

1. Introduction

Mesopotamia is a key region for the archaeology of the Middle East. Geomorphological and to a lesser extent geological investigations have been undertaken since the early 20th century to reveal the Holocene sedimentary development of the low-lying plain. The major points of interest of the researchers were related to the anthropogenic impact on the landscape changes, and the sea-level history of the Persian Gulf. However, all investigations were carried out in the Iraqi part of Mesopotamia. For an overview, see Baeteman et al. (2004/2005), Heyvaert and Baeteman (2007) and Bogemans et al. (2017). The Lower Khuzestan plain in SW Iran, however, also belongs to Mesopotamia. Here proper geological investigations like in Iraq were non-existent, and the sometimes contrasting ideas about the development of the plain were inferred from historical sources and surface observations.

In an attempt to meet this void the Holocene depositional evolution and in particular the extension of the Persian Gulf has been investigated in a project combining geo-environmental reconstructions and archaeological data in the Lower Khuzestan plain (Baeteman et al., 2004/2005; Gasche and Paymani, 2005; Heyvaert and Baeteman, 2007). The plain was hitherto an uncharted territory; therefore a large area was surveyed. The study area extended from the Persian Gulf to the Ahwaz and Agha Jari anticlines (Fig. 1). It was surveyed by means of 54 hand-operated cores reaching depths between 4 and 7 m. The results of this project showed that the Persian Gulf extended at least 80 km north of the present coastline at around 8000 yr cal BP. Tidal flats developed and shifted rapidly inland. Until 7000 yr cal BP the lower lying areas were largely wetlands sensitive to inundations by estuaries and rivers. The intertidal environments evolved into salt marshes as a result of the rapid sea-level rise in combination with a high sediment input. The palaeogeographical maps show a tidal flat environment as far as 120 km north of Khorramshahr. The abundance of evaporites in the sedimentary record made the authors conclude that coastal sabkhas replaced the salt marshes indicating a climate change toward a more arid setting probably around 4500 cal BP, an age that was put forward by Aqrawi (2001). Around 1350 - 1250 yr cal BP according to Baeteman et al. (2004/2005) but around 2500 yr cal BP

* Corresponding author.
E-mail address: frieda.bogemans@naturalsciences.be (F. Bogemans).

http://dx.doi.org/10.1016/j.quascirev.2017.07.011
0277-3791/

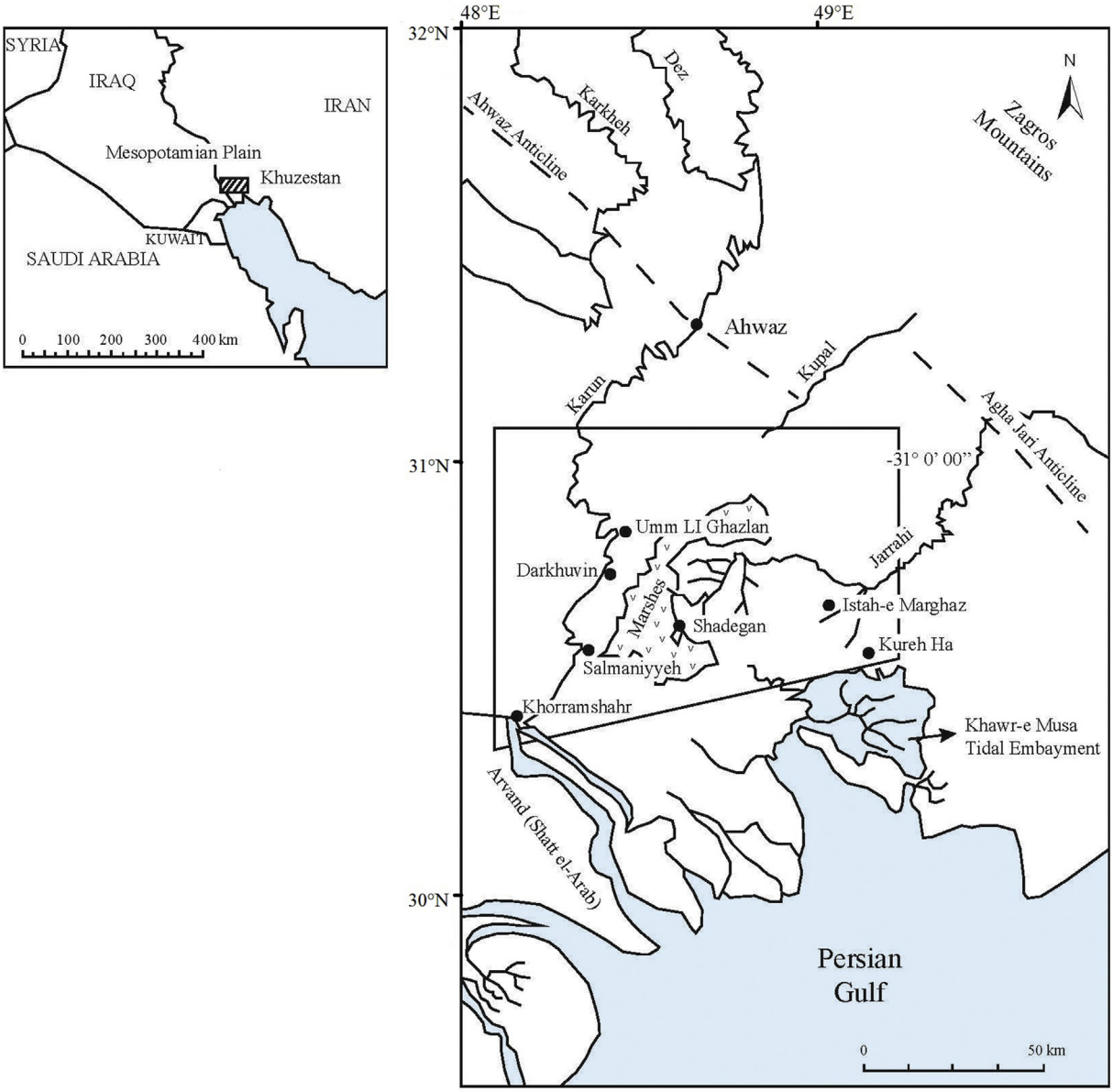

Fig. 1. General location of the study area in relation to the Persian Gulf and neighbouring countries with indication of the cited cities in the text.

according to Heyvaert and Baeteman (2007) the coast started to prograde whereby the sabkhas were replaced by a floodplain.

The contribution and impact of the fluvial systems on the depositional environments, however, was not sufficiently acknowledged. The major part of the Holocene record was interpreted as tidal deposits, despite the ubiquitous presence of the rivers Karun and Jarrahi in the landscape in this part of the Lower Khuzestan plain (Fig. 1). With respect to the rivers, additional investigations have been carried out using remote-sensing techniques and textual sources (Verkinderen, 2009; Walstra et al., 2010a, 2010b; Dupin, 2011). These studies, investigating mainly the impact of human activities on the landscape, were restricted to the detection of changing watercourses since antiquity, and did not discuss the evolution of the depositional environments during the Holocene.

To investigate the Holocene depositional evolution of the Lower Khuzestan plain a joint project with the Geological Survey of Iran was launched in 2013. The objective was to determine the effect of terrestrial and littoral processes as well as the impact of external forces on the nature and dynamics of the sedimentary systems. Therefore, the southern part of the Lower Khuzestan plain, where during the Holocene terrestrial and littoral processes met and interacted, was selected as study area. This paper presents the results of fieldwork campaigns carried out in 2013, 2014 and 2015 revealing the reconstruction of the sedimentary environmental evolution since the end of the Late Pleistocene, but with the main accent on the evolution during the Holocene.

2. Setting

The study area belongs to the Mesopotamian Plain, a large foreland basin of the Zagros Mountains (Sharland et al., 2001; Konyuhov and Maleki, 2006). The Zagros Mountains, located northeast of the area, originated from the collision of the Arabian and Eurasian plates. They are the sediment source of the rivers Karun, Kupal and Jarrahi. The Zagros Mountains and the Khuzestan plain are characterized by a very intense seismicity, but the seismic magnitude is low. Consequently the created deformations are

predominant aseismic (Masson et al., 2005; Hatzfeld et al., 2010; Woodbridge et al., 2015).

The study area is situated in the southwestern part of the Lower Khuzestan plain between Khorramshahr and Kureh Ha in the south, and the 31°0′0″N (WGS, 1984) latitude in the north (Fig. 1). The major part of the study area has a flat topography with an altitude between +3 m and +5 m msl (mean sea level). The topography rises towards the north and east reaching +13 m msl in the east, which is the highest level measured in the survey area. Within the Shadegan area, east of the Shadegan marshes, the topography is slightly undulating, with an altitude ranging between +3 and + 9 m msl. The areas above +5 m msl are in general agricultural land.

The rivers Karun and Jarrahi cross the area and some ephemeral branches of the Kupal river touch the northern boundary of the study area. The rivers cut transverse through the well-developed folds in the Zagros Mountains via deep incised valleys (Setudehnia and O'B Perry, 1966 - Geological maps Marun, 20830 W and Haft Kel, 20830 E, scale 1/100 000; Woodbridge et al., 2015). The Jarrahi river has no direct connection with the sea; water and sediments debouch in the marshes of Shadegan. The marshes drain via the Khawr-e Musa tidal embayment (Fig. 1). The water of the Kupal river is artificially diverted into irrigation canals once it enters the Lower Khuzestan plain. At the southwestern border of the study area the river Karun, which is the major river in Iran, discharges into the Arvand (Shatt al-Arab) that in turn flows into the Persian Gulf. Ninety percent of all sediments in the Arvand is brought in by the Karun river, the other ten percent is coming from the Tigris and Euphrates rivers (Encyclopaedia Iranica - http://www.iranicaonline.org/). Nowadays tides progress inland via the Karun till Darkhuvin (Adib, 2010). The average tidal range is 2.5–4 m along the coast (United Kingdom Hydrographic Office, 2005; Encyclopaedia Iranica - http://www.iranicaonline.org/) and reaches around 3 m in the Karun near Khorramshar (Adib, 2008). Except along a few channels in the south, the study area is out of tidal reach and solely continental processes control sedimentation. The groundwater level fluctuates between 0.25 m and 2.35 m below the surface (personal communication Reza Shahbazi – Geological Survey of Iran).

3. Methods

Fieldwork consisted of sixty-six hand-operated gouge cores attaining depths up to 12 m and resulting in a good coverage (Fig. 2). The cores were described directly in the field. The description includes texture, sedimentary structures and bedding-plane characteristics, colour, the presence and nature of palaeontological remains, presence and type of evaporite crystals, relative degree of consolidation and pedological features. Per core a litholog was drawn on basis of the field descriptions and assembled in several N-S and W-E transects, to define the core-to-core relation

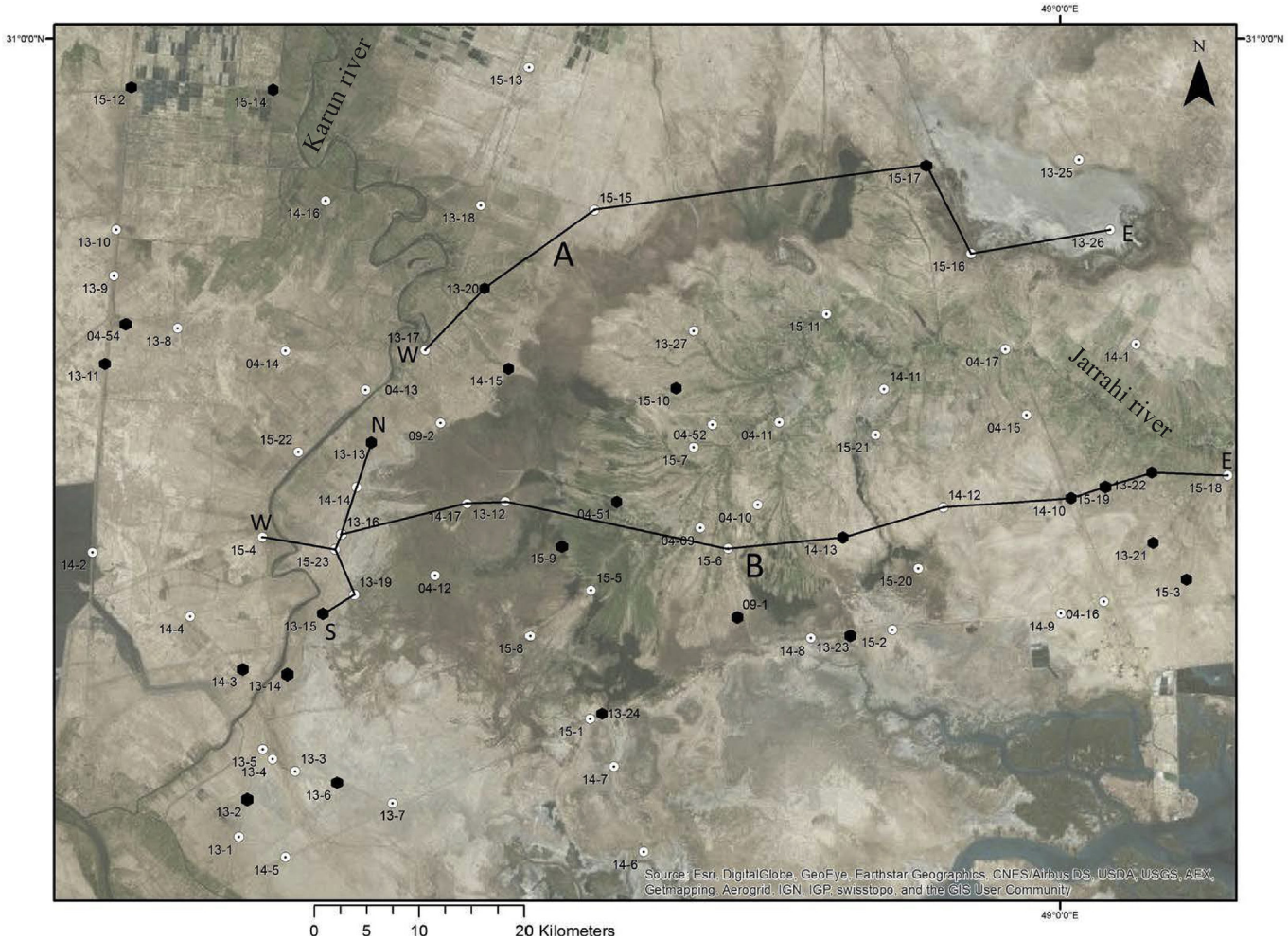

Fig. 2. Location map of the boreholes and the three transects shown on Figs. 3–5. The Shadegan marshes with the mouth of the Jarrahi river are well displayed in the centre of the map. A black octagon indicates the radiocarbon sampling sites.

Table 1
Description of the lithological units introduced in this study.

Unit code	Textural composition	Sedimentary characteristics
S1	Fine to medium sand	Predominant homogeneous Locally fine siliciclastic lenses, laminae, beds Occasionally few very small fragments of molluscs
S2	Fine sand, silty fine sand, sometimes medium sand	Massive as well as stratified Clay/silt laminae and lenses Cemented sand grains, up to a diameter of very coarse sand
Si	Very fine and fine sand	Laminae or thin beds of silty clay or clay, scattered over the unit and/or deposited as an interlayered set. A set is maximum a few dm thick Occasional bioturbations Occasional shell fragments, either concentrated or spread over the unit
[S-F]i	Complex composed of laminae and beds of mud (clay, silty clay or clayey silt) and fine sand	Irregular layered along (sub)horizontal and oblique planes Remnants of roots and vegetation may be present along with traces of bioturbation, desiccation cracks and signs of preliminary pedogenesis
[S-F]a	Alternating complex of mud (silty clay, silt or clay) and fine sand	Deposited as laminae and/or thin beds in both a regular or irregular pattern. Locally deformation structures, mostly load casts and slump structures, may be present. Locally shell fragments occur but not in large quantities Occasional bioturbations
Fi	Clay and silty clay	Laminae of fine sand or silt. (Sub)horizontal stratification is dominant. Only small quantities of shell remnants as well as organic matter occur.
F1	Clay and silty clay, sometimes silt	Massive structured Vegetation remains may be present but not an a regular base Occasional complete or broken mollusc
F1(sh)	Clay and silty clay, sometimes silt	Massive structured Unbroken gastropods and/or complete disarticulated bivalves, subordinate fragments Vegetation remains may be present but not an a regular base
F2	Clay and silty clay, sometimes silt	Massive bedding prevails but the unit may be interlayered with silt to fine sand laminae, small beds or lenses Occasional clay pellets, often very stiff Occasional organic debris and mollusc fragments
F2(sh)	Clay and silty clay, sometimes silt	Massive bedding prevails but the unit may be interlayered with silt to fine sand laminae, small beds or lenses Mollusc fragments, concentrated or scattered in the sequence Occasional clay pellets, often very stiff Occasional organic debris
F3	Clay and silty clay, less common clayey silt and silt	Massive structured Thin beds and/or thick laminae of amorphic vegetation remains, rests of microbial mats, dots and small lumps of organic litter and root remnants, scattered over the unit or concentrated in sets Complete gastropods and fragments of both bivalves and gastropods occur Occasional calcareous tufa

and to obtain a spatial overview. Three transects are presented here, though simplified. The core descriptions are supported by bulk XRD analysis of 127 samples representing the semi-quantitative main mineralogy: palygorskite, gypsum, total clays (illites, smectites and kaolinites), aragonite, calcite, dolomite, quartz, K-feldspar and plagioclase, and to a lesser degree halite. Boreholes are located using a handheld Dakota-20 Garmin GPS with a horizontal precision of maximum 15 m. The altitude is inferred from NASA SRTM (NASA JPL, 2013). In Iran the ordnance datum equals mean sea level (msl) (http://www.trigtools.co.uk/datums.cgi?rows%3d1%26cols%3d1).

In the scope of creating a timeframe for the depositional environmental evolution, radiocarbon datable material was sampled (Fig. 2). All samples were collected in fine-grained sediments and consist of organic amorphic matter of plant origin, roots, microbial mats and molluscs. The radiocarbon analysis was done by Accelerator Mass Spectrometry (AMS) at the Royal Institute for Cultural Heritage (Brussels). The results are presented as conventional radiocarbon ages and calibrated ages (Tables 3 and 4). The interpretation of the radiocarbon data is dealt with caution in this area because the dated material may have been subject to contamination by older carbonates supplied by both the Gulf water and river water. The recognition and understanding of the problems related to the carbon reservoir effect was discussed in Bogemans et al. (2017).

Table 2
The lithological units in relation to the sedimentary subenvironments and environments.

Lithological units	Sedimentary subenvironments	Sedimentary environments
F1, F2, F1(sh)	Supratidal	Estuarine, fluvial-estuarine, upper delta plain (ES, F/D)
F1, F3, [S-F]i, Fi, [S-F]a	Pond, shallow lake	Fluvial, upper delta plain (M1, M2, F/D)
F1, F2, F3, F1(sh), [S-F]i, S2	Overbank forms, within channels forms	Fluvial, upper delta plain (M1, M2, MX, F/D)
Fi, [S-F]a, F2, F2(sh)	Intertidal	Estuarine (ES)
[S-F]a, Si	Subtidal	Estuarine (ES)
S1, S2	Within channels forms, sand sheet	Fluvial (S)

Table 3
Radiocarbon dates obtained from organic matter. The samples are calibrated using Oxcal 3.1 and the INTCAL13 calibration curve (Bronk Ramsey, 1995, 2001; Reimer et al., 2013). Ages are given with a 2-sigma error range in calendar years BP.

Core number	Laboratory code	Material	Depth msl (m)	Age BP	Calibrated age BP
14–13	RICH-21187	Organic matter	+5.20	588 ± 32	530–660
15–14	RICH-22084	Organic matter (condensed amorphic matter)	+4.79/+4.88	1580 ± 31	1400–1550
13–21	RICH-20355	Organic matter (condensed amorphic matter)	+2.40	2034 ± 32	1890–2070
15–19	RICH-22069	Organic mud	+3.10/+3.15	7885 ± 42	8580–8980
14–10	RICH-21186	Organic matter	+3.06/3.15	4567 ± 40	5200–5450
04-51*	KIA-26480	Organic matter	+2.75	280 ± 20	350–430
13–22	RICH-20374	Organic matter (patches - not in situ)	+2.70	5037 ± 32	5710–5900
13–22	RICH-20356	Organic matter (condensed amorphic matter)	+2.60/+2.70	2062 ± 31	1940–2130
13–23	RICH-20357	Organic matter	+2.50	4292 ± 33	4820–4970
15–9	RICH-22083	Peaty mud	+1.85/+1.87	586 ± 30	530–660
14–15	RICH-21190	Organic matter (condensed amorphic matter)	+1.60/+1.63	879 ± 32	720–920
13–13	RICH-21189	MMs	+1.60	7001 ± 42	7730–7940
13–13	RICH-20375	Organic matter (condensed amorphic matter)	+1.25	10354 ± 43	12.040–12.400
13–15	RICH-20376	Organic matter (condensed amorphic)	−2.75	6729 ± 32	7510–7670
13–15	RICH-20348	Organic matter (condensed amorphic/MMs)	−3.27	7078 ± 36	7830–7980
04-54*	KIA-26482	Organic matter (root)	−3.6/-3.7	6980 ± 35	7710–7880
04-54*	KIA-26746	Organic matter (root)	−3.75/-3.8	7275 ± 35	8010–8170
13–11	RICH-20347	Organic matter (root)	−4.3/-4.36	6882 ± 37	7620–7800
14–15	RICH-21191	Organic matter (condensed amorphic)	−4.46/-4.51	7618 ± 42	8360–8520
13–20	RICH-21193	Organic matter (patches - not in situ)	−5.18	11058 ± 53	12.780–13.070
13–14	RICH-20349	MMs	−5.22	7030 ± 37	7780–7950
04-54*	KIA-26747	Peaty mud	−5.4	7085 ± 35	7840–7980
13–24	RICH-20358	Organic matter (plant remnants)	−5.52	7222 ± 36	7960–8160
13–24	RICH-20359	Organic matter (strongly decomposed)	−5.80	7104 ± 37	7850–8010
14–3	RICH-21185	Organic matter (plant remnants)	−7.42/-7.46	9593 ± 48	10.740–11.150

* Data from Heyvaert and Baeteman (2007).

Table 4
Radiocarbon dates obtained from molluscs. The aquatic molluscs are calibrated using Calib 7.1 and using the MARINE13 calibration curve with a reservoir age correction ΔR of 190 ± 25 (Bogemans et al., 2017). Ages are given with a 2-sigma error range in calendar years BP.

Core number	Laboratory code	Material	Depth msl (m)	Age BP	Calibrated age BP	δ13 C (‰)
13–6	RICH-20324	Molluscs (not in situ)	+4	4175 ± 31	3862–4116	−0.6
15–10	RICH-22033	Molluscs (in situ)	+2.9/+3.1	2428 ± 30	2350–2700	−6.8
13–6	RICH-20325	Molluscs (not in situ)	+2.77	4065 ± 30	3710–3960	+1.0
09–1	KIA-43036	Molluscs (oysters)	+2.1/+2.04	5610 ± 10	5669–5900	+1.42
13–2	RICH-20302	Molluscs (not in situ)	+1.85	4310 ± 31	4055–4336	−1.0
13–14	RICH-20326	Molluscs (not in situ – bivalve)	+0.74	4318 ± 30	4067–4338	+0.9
13–6	RICH-20303	Molluscs (not in situ)	−0.45	5027 ± 31	4990–5274	?
15–12	RICH-22032	Molluscs (in situ)	−3.39/-3.42	7508 ± 37	7672–7894	+1.0
13–15	RICH-20345	Molluscs (in situ Cerithidae)	−3.80	7868 ± 36	8014–8263	−0.8
15–12	RICH-22034	Molluscs (in situ Cerithidae)	−3.95	7693 ± 38	7851–8075	+1.3
13–24	RICH-20327	Molluscs (not in situ	−6.2/-6.5	8595 ± 36	8852–9143	−1.9

4. Data and results

Water-laid deposits prevail in the sediment records; they accumulated in terrestrial and tidal environments under ephemeral and perennial conditions. Eleven lithological units have been discriminated. The units are identified on basis of texture and completed with primary depositional attributes and specific but recurrent sedimentary properties. The detailed description of the units is shown in Table 1. All deposits in the area are calcareous. They have a stiff, firm and/or soft consistency, but no correlation to a specific lithological unit or stratigraphic position is observed. Even within one unit, the degree of consolidation can change. Soft sediments are in general greyish coloured whereas the firm and stiff deposits do not have a specific colour. Colour change due to oxidation and reduction are both observed. The reconstruction of the successive sedimentary environments has made use of (i) the association of the lithological units in vertical successions (Table 2), and (ii) their distribution and stratigraphic position (Figs. 3–5).

4.1. Fluvial environment

On the basis of the textural properties, most of the fluvial deposits are classified as mud-dominated and sand-dominated deposits, independently of the architectural element they belong to. Furthermore, dependent on the depositional characteristics and their stratigraphic position, two variants are recognized within the mud-dominated rivers deposits. On top of the sand-dominated river deposits a heterolithic mud - sand facies exists although infrequently.

4.1.1. Sandy fluvial deposits with a heterolithic topset

The sand deposits “S” are uniformly structured, and consist exclusively of the sand unit S1 showing a greyish less common light brownish colour. Depositional sequences of more than 8 m are recovered in the area; the base is nowhere reached. The deposits map out as buried ridges, predominantly N – S orientated (Fig. 3), with in-between depressions. The crests of the ridges are slightly dipping towards the south. Locally the ridges are dissected by younger sedimentary systems (Fig. 5).

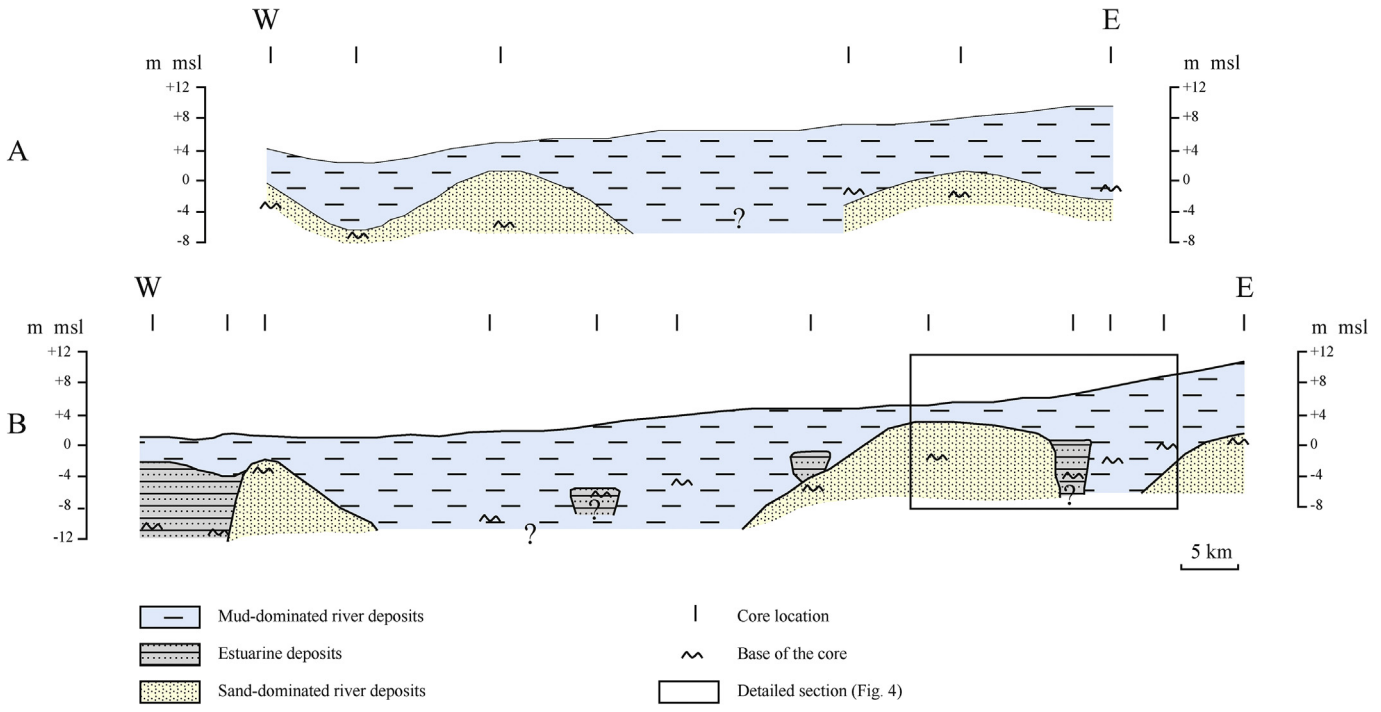

Fig. 3. Two schematic west-east oriented transects respectively located in the distal (A) and proximal position (B) relative to the Persian Gulf. Their location is shown on Fig. 2. The transects clearly show the presence of the Late Pleistocene sand ridges all over the study area, and the absence of estuarine deposits in the distal part (A).

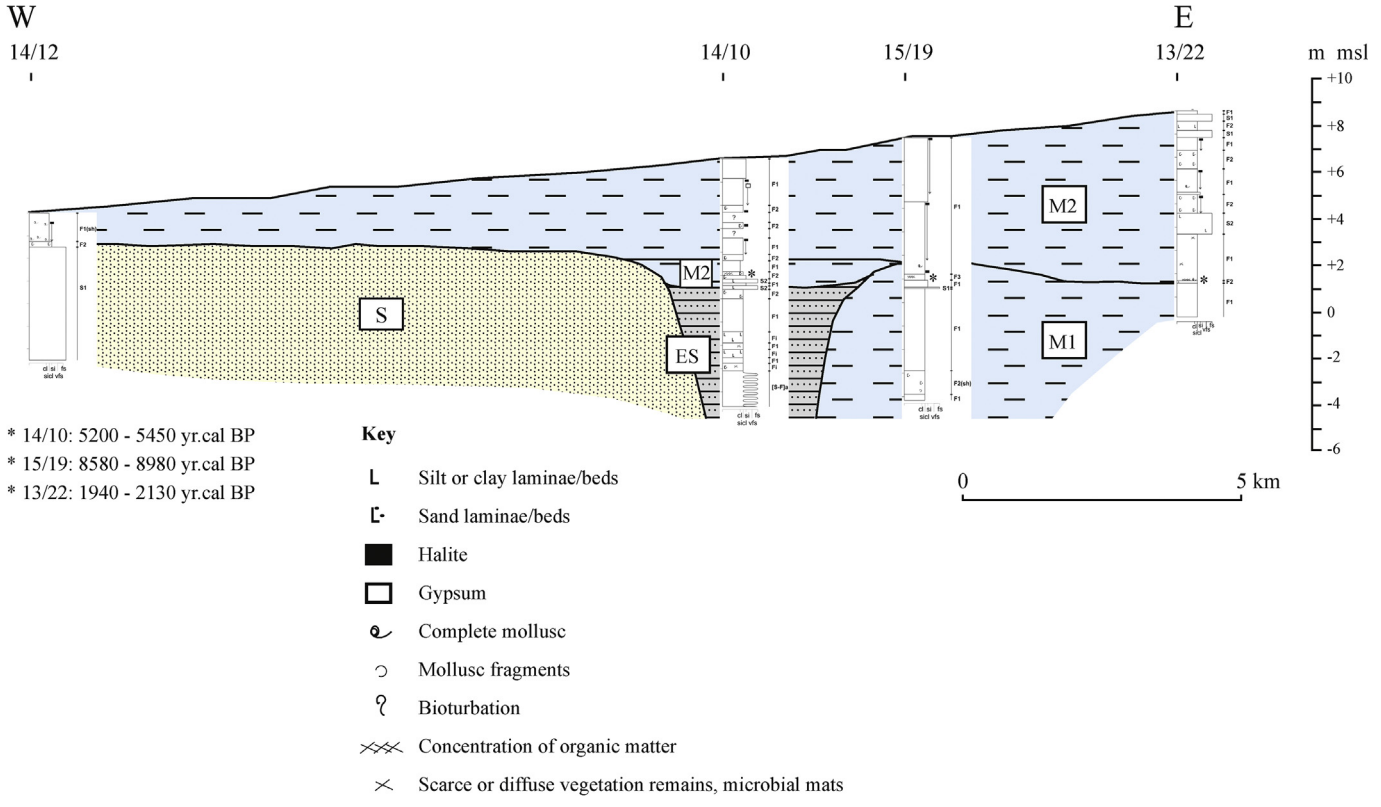

Fig. 4. An enlarged part of section B shows the distribution of the lithological units and the depositional environments in the Jarrahi basin. The section shows the depression in which the estuary invaded inland. A local erosional surface was detected at the top of the estuarine infill in core 14/10. The difference in radiocarbon ages of the samples located at about similar depths demonstrates the complex evolution in the development of the plain. See Fig. 5 for the symbols of the depositional units.

In few isolated niches heterolithic deposits "MX", consisting of the units S2, [S-F]i and F1 are present on top of the sand-dominated river deposits (Fig. 5). The sedimentary characteristics are typical for natural levee or point bar deposits covered by floodplain deposits. Early soil development, desiccation cracks and traces of plant roots are common in the top part. In

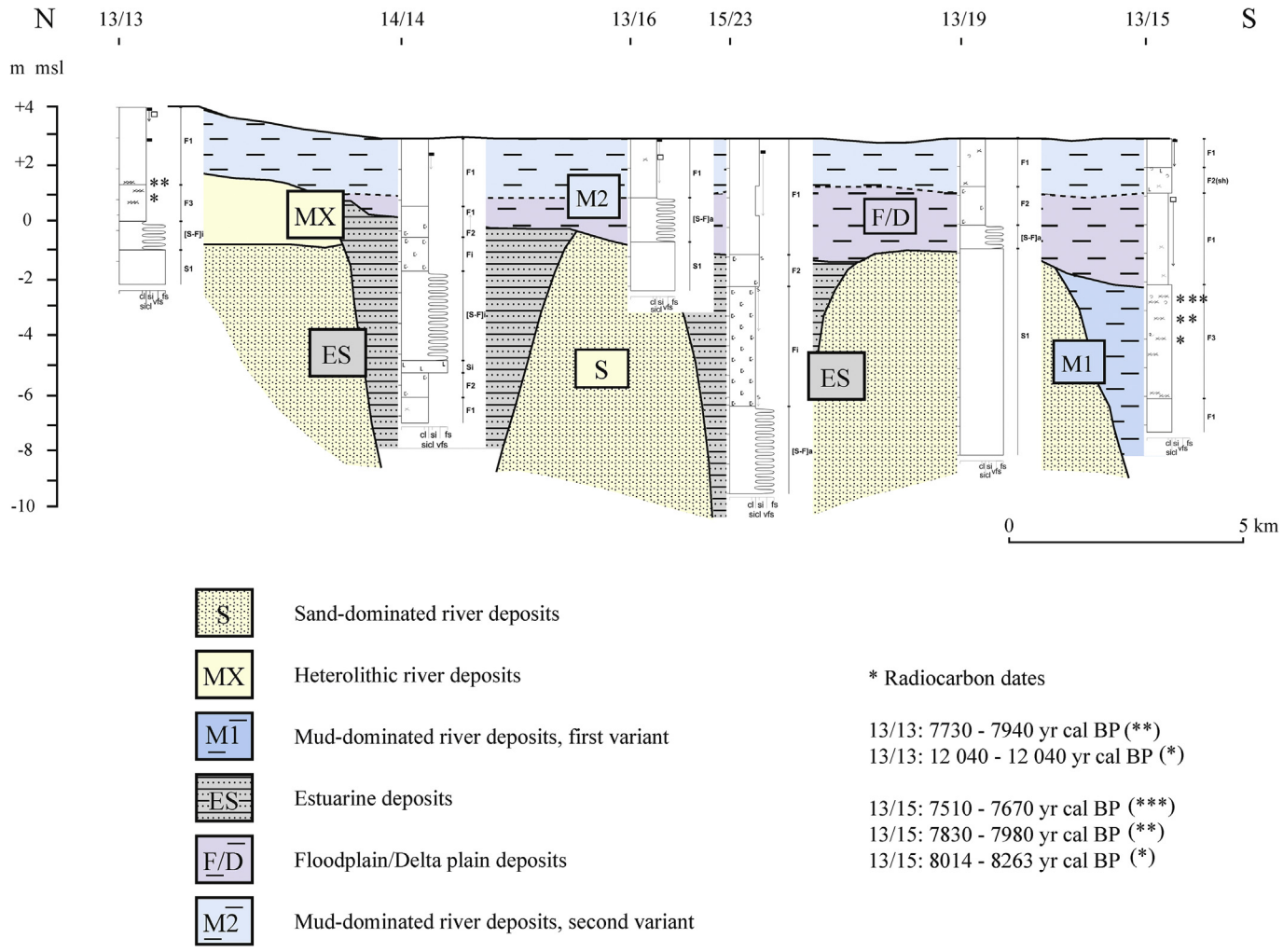

Fig. 5. The detailed N-S section adjacent to the Karun river shows ridges composed of predominant sand-dominated river deposits and depressions filled with estuarine deposits in the north and deposits of the first variant of mud-dominated rivers in the south. The incision of the two northern depressions post-date the southern one. The presence of the heterolithic deposits as a topset of the sand-dominated river deposits is only observed in core 13/13. In the rest of the transect, but approximately at the same depth, younger upper delta plain deposits cover the depression fills and the sand-dominated river deposits. The surface layer consists of the second variant of mud-dominated river deposits. See Fig. 2 for location of the transect and Fig. 4 for the core key.

core 13/13 the deposits near the top are dated to 12400 - 12040 yr cal BP (Table 3).

4.1.2. Mud-dominated river deposits

Two variants of mud-dominated river deposits were found, each occupying a specific stratigraphic position within the sequence, the second variant occurring in a shallower stratigraphic position. The first variant "M1" is both greyish and brownish coloured and is characterized by a predominance of F3 deposits in association with sediments of the F1 unit. F1 sediments are prevalent in the basal part of this depositional record (Fig. 4). Less frequent are the units F2 and S2, the latter having commonly a maximal thickness of a few decimetres. Where sand-dominated river deposits are lacking, these mud-dominated river deposits take usually the lowermost position within the core records. Organic matter as typical characteristic of F3 is less abundant in the most northern and eastern part of the study area (Fig. 4). Most ages are clustered in the interval 8150 - 7750 yr cal BP, with an outlier dated to 7670 - 7510 yr cal BP (Table 3).

In the second variant of the mud-dominated river deposits "M2" F3 is a minor component. S2 deposits have become a defining element in the northern and southeastern border region of the study area. Away from these regions, the number and thickness of the sand strata decreases, and the fluvial record is essentially composed of the fine-grained units F1 and F2 (Fig. 4). In these latter units broken or complete molluscs of *Lymnaea auricularia*, *Melanoides* and *Cerithidea* occur, especially in the central part of the study area, sometimes in combination with organic matter of plant origin. The different molluscs in Table 4 have not been classified into freshwater, marine and brackish species because e.g. species known as marine can also inhabit terrestrial environments where salinity is sufficiently high (see discussion in Bogemans et al., 2017). Light brownish and yellowish colours are common, often alternating with gleyic coloured zones. Thick pure grey coloured layers are exceptional. Radiocarbon ages of this variant come mainly from a region that nowadays is part of the Jarrahi alluvial plain, except the samples 14/15 and 15/14. All ages are younger than 3000 yr cal BP. Two samples collected from the basal part of these deposits have an age around 2000 yr cal BP (Table 3: cores 13/21 and 13/22). Organic matter present in the upper part is dated to 1550 - 1400 yr cal BP in the northwest (Table 3: core 15/14) whereas an upper lying sample taken at the margin of the Shadegan marshes has an age of 920–720 cal BP (Table 3: core 14/15). Three of the four samples collected in the Shadegan area give an age between 660

and 350 yr cal BP, unrelated to their altitude (Table 3: cores 14/13, 04/51 and 15/9). The fourth Shadegan sample is dated to 2700 - 2350 yr cal BP (Table 4: core15/10).

4.2. Tidal environments

The tidal deposits in the study area are interpreted as estuarine deposits since they cover only narrow parts within the incised depressions and their thickness as well as the sand content decrease land inwards. Most of the preserved estuarine deposits "ES" belong to a subtidal and intertidal environment. The subtidal deposits are mainly composed of the greyish coloured units Si and [S-F]a; the intertidal deposits consist essentially of the grey to light browngrey coloured units F2, Fi, [S-F]a, [S-F]l (Figs. 4 and 5). The tidal deposits in the sediment record occur as far as Umm Ul Ghazlan in the Karun basin, and Istah-e Marghaz in the Jarrahi basin (Fig. 1). Useful radiocarbon dating is almost non-existent. Only a bed of in situ oysters in core 09/1 provided the opportunity to get an age determination of 5900–5669 yr cal BP (Table 4). Two broadly similar radiocarbon dates of the base of "M2-F/D", lying directly on top of the estuarine deposits, and dated to 5450 - 5200 yr cal BP (Table 3: core 14/10) and 4970 - 4820 cal BP (Table 3: core 13/23) give a minimum age indication of the general termination of the tidal influences in the area (circa 5.3 ka cal BP; Fig. 6).

4.3. Observations related to evaporites

The main evaporite minerals observed in the cores are gypsum and halite. These evaporites, which are not diagnostic for a specific environment, occur in both fluvial and tidal environments and do not show a specific distribution pattern. It is however noteworthy that the deposits of the second variant of the mud-dominated rivers ("M2") are the most enriched. Fine siliciclastic sediments usually act as host deposit. Halite is generally found in firm and stiff clay and silty clay as individual crystals, clustered in small nodules (few mm) or veins, but not as a crust except at the surface. Gypsum is widely observed as individual crystals, currently few centimetres long, and their long axis is vertically oriented. The bulk XRD results show that in most cores, unrelated to depth, a small amount of gypsum is present. The major part of gypsum crystals occurs above ca −2 m msl. Halite occurs in general higher up in the core records. Pursuant to the different brine concentration needed for the formation of halite and gypsum, it is obvious that they are in inverse relation in the records.

5. Discussion

5.1. Evolution of the study area since the end of the Late Pleistocene

In this study the subdivision of the Holocene as proposed by Walker et al. (2012) is used; the early–mid-Holocene boundary is placed at 8200 yr BP, the mid–late Holocene boundary at 4200 yr BP.

The sedimentary characteristics of the oldest recovered deposits reveal the presence of a fluvial environment at the end of the Late Pleistocene. Their thick and in particular uniform lithological sequence documents such palaeohydraulics whereby depositional and preservational processes allow only aggradation of sand deposits ("S"). This palaeohydraulic situation changed prior to 12400–12040 yr cal BP and fine-grained deposits became part of the fluvial depositional environment and even turned into a dominant facies. Point bars and/or natural levees evolving into a fine-grained floodplain then characterized the fluvial environment ("MX"). This situation lasted at least until 12400 - 12040 yr cal BP, because the dated sample was collected just below the top of the floodplain deposits (Fig. 5, core 13/13). The very top of the deposits could not be dated. Presumably, shortly after an erosional phase started. It extended across the whole study area and several depressions were created. The not eroded sand and heterolithic deposits were left as ridges in the landscape. Those ridges acted later on as divides. From then each depression hosted a river, today known as the Karun (in the west), the Kupal (in the centre) and the Jarrahi (in the east) rivers. Although radiocarbon data are limited, these data in combination with their stratigraphic position place the erosional event post 12400–12040 yr cal BP but prior to

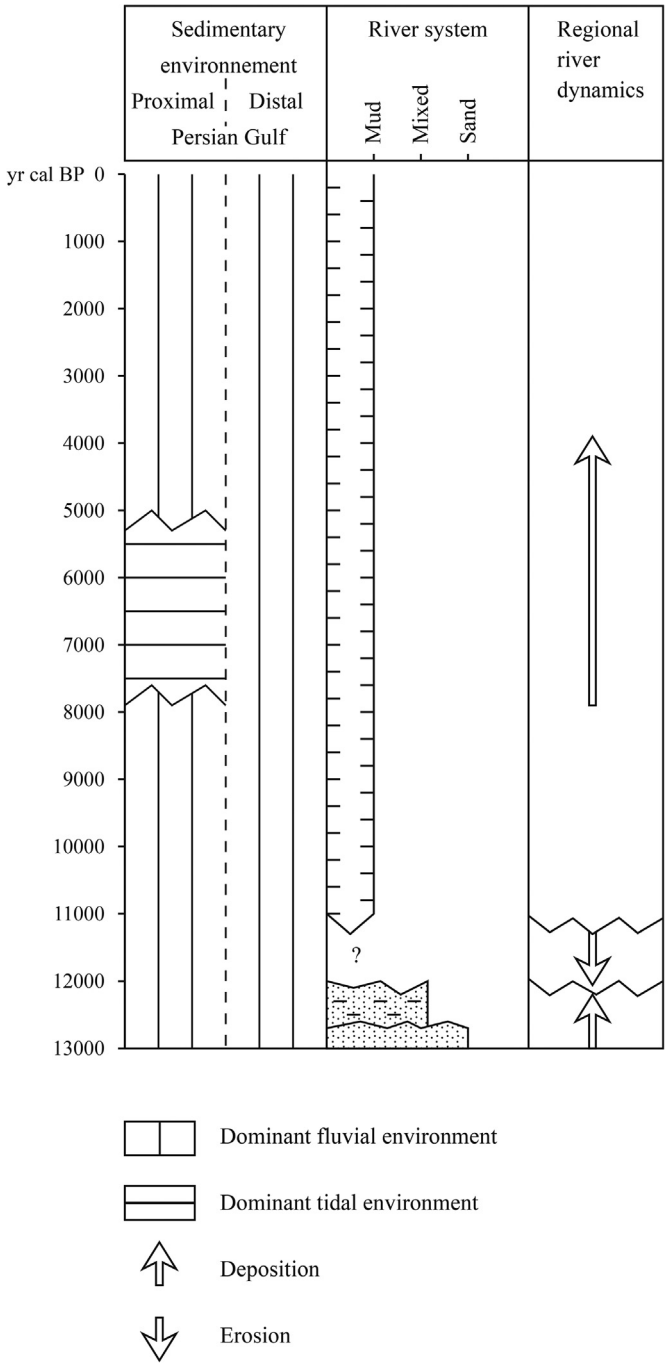

Fig. 6. Compilation of the sedimentary environments since the end of the Late Pleistocene, types of rivers and their dynamics, and observed changes of the effective wetness showing a difference between the proximal and distal position of the study area to the Persian Gulf.

11150–10740 yr cal BP (Table 3: cores 13/13; 14/3). The first age dates the floodplain deposits, which mark the former surface; the latter age dates the start of the infill of one of the newly incised depressions. The early Holocene age for the start of the infill is indirectly sustained by the fact that the sediments dated between 8150 and 7750 yr cal BP are lying above several metres of clay deposits. This has been observed in several cores in each depression. Consequently, we assumed that the erosional phase happened during the Younger Dryas (12700 - 11560 yr cal BP).

The infill of the depressions was first controlled by mud-dominated rivers (Fig. 6). Their predominance lasted a few thousand years, at least until 7900–7700 yr cal BP. In this fluvial environment rather poorly drained alluvial plains suitable for vegetation growth were not exceptional (Bogemans et al., 2017). After that date, the sedimentary environment in the area adjacent to the Persian Gulf was directly affected by the Holocene sea-level rise (Fig. 6). Tides invaded inland via the existing channels and eroded at least part of the mud-dominated river deposits (Figs. 4 and 5). This is in contrast with the current idea that the Holocene sea-level rise resulted in the flooding of the entire plain as shown on the figures published by e.g. Sanlaville (1989), Pournelle (2003), Sanlaville and Dalongeville (2005), Kennett and Kennett (2006, 2007), Day et al. (2012). Sedimentary evidence shows that as the sea-level rise continued, the tidally influenced Karun estuary reached as far as Umm Ll Ghazlan and expanded also laterally in the area adjacent to the Gulf (Bogemans et al., 2017). Although nowadays the river Jarrahi has no direct connection to the Persian Gulf, our data prove that the Jarrahi river joined the Gulf via an estuary during the mid-Holocene and tidal deposits reached as far as Istah-e Marghaz (Figs. 1 and 4). In between the Karun and Jarrahi depressions another depression existed which comprised two tidal branches, most probably belonging to the proximal part of the Kupal (Fig. 4). The data suggests that the Kupal and Karun belts merged south of Salmaniyyeh. The landward part of the study area on the contrary stayed out of tidal influences and was continuously controlled by terrestrial processes during the whole Holocene (Figs. 3 and 6). These results show that the conclusions by Baeteman et al. (2004/2005) and Heyvaert and Baeteman (2007) need adjustment. The idea of a far northward extension of the Persian Gulf around 8000 yr cal BP has to be abandoned because the tidal invasion extended only slightly further northwards than Darkhuvin in the Karun basin, and stopped nearby Istah-e Marghaz in the Jarrahi basin. Also the overall distribution of tidal flat deposits in the entire study area as suggested by the previous investigations must be reviewed. The tidal flat deposits were confined to the estuaries; no tidal embayment was present. The idea of a far northward extension of the tidal environment during the mid-Holocene arose from the results of microfossil analyses of the soft blue-grey mud in the north showing brackish-marine diatoms and foraminifera similar to those occurring in intertidal and estuarine environments (Heyvaert, 2007).

The period during which tidal processes controlled the southern part of the area could only be determined indirectly. The alluvial plain overlying the tidal deposits has been dated to 4970 - 4820 yr cal BP at the southern margin of the study area (Table 3: core 13/23), and to 5450 - 5200 yr cal BP nearby Istah-e Marghaz about 20 km more to the northeast (Table 3: core 14/10). On the whole it can be said that the tidal invasion that lasted for about 2000–2500 years, stopped around 5000 yr cal BP because fluvial processes steered the evolution of the sedimentary environment again and progradation started (Bogemans et al., 2017). However, proper delta deposits, which would be the evidence for a progradation (cf. Dalrymple, 1992; Dalrymple et al., 2003) have not been found; only relicts of a delta plain seem to occur in the subsoil of the study area. Lateral and vertical interrelations between shallow lacustrine and fluvial deposits (e.g. Fig. 5: core 13/19) are in support of the existence of an upper delta plain ("F/D"). Also evidence of temporary channels under tidal influence younger than 4000 yr cal BP (Table 4: cores 13/2 and 13/14) downstream Salmaniyyeh may point to the existence of a lower delta plain. In the very south tides control locally the sedimentary environment.

During the second half of the mid-Holocene vegetation diminished, evaporitic crystals were formed frequently though irregularly, and well-drained conditions were present. Therefore it is assumed that the effective wetness decreased. This may be caused by factors like a decline in precipitation, an increase of evaporation, a decrease in wetness and/or an increase of seasonality (Jones et al., 2013). The occurrence of sand strata in the upstream part of the study area may point to an increase of seasonality. Because they are absent in the downstream area, high-magnitude extreme flood events seem to be unlikely. In addition, other characteristics like the scarce vegetation and the presence of evaporitic crystals suggest also a reduction of effective moisture. However, an accurate time determination is not possible for the moment being due to lack of data.

Baeteman et al. (2004/2005) and Heyvaert and Baeteman (2007) stated on basis of the presence of secondary gypsum growth that coastal sabkhas replaced the salt marshes. However, the independency of the evaporites to any environment as well as their more frequent occurrence in the mid-to late Holocene mud-dominated river deposits, demonstrate that the interpretation of the existence of a coastal sabkhas in the study area is incorrect.

5.2. Climatic impact on the fluvial environmental changes

The controlling force behind the erosive event that took place during the Younger Dryas had most probably an external cause because the incision happened simultaneously in the lower part of the Karun, Kupal and Jarrahi basins. The result was the development of three depressions. It is widely accepted that in natural circumstances tectonics and climate are the main external key factors triggering fluvial environmental changes (e.g. Knighton, 1984; Miall, 1996; Blum and Törnqvist, 2000). But as tectonic movements are predominantly aseismic in the survey area its triggering effect is negligible. A base level lowering could also have caused an incision since the study area is located nearby the Persian Gulf. However, a downcutting implies a lowering of the base level, which in the case of the Persian Gulf is most unlikely because of the impact of the rising sea level at the final stage of the Late Pleistocene.

The impact of a local base level change induced by the Tigris-Euphrates system is also not possible because the depressions of the Karun, the Kupal and the Jarrahi had a north-south orientation and could by no way be tributaries of the Tigris-Euphrates system during that period. Therefore, a climate change caused most probably the disequilibrium state that led to incision. All available data in Iran indicate a drier climate during the Younger Dryas (Wasylikowa et al., 2006; Kehl et al., 2009; Pickarski, 2013). This information in combination with the knowledge that an arid area has a high potential for extensive erosional events (Nanson, 1986; Molnar, 2001; Molnar et al., 2006) especially when climate further aridifies, sustain our statement.

The transition from a dominant erosional to a dominant depositional fluvial environment during the early Holocene is most probably also forced by a climate change. There is definitely evidence of climate changes during the Holocene in Iran but because of the vast extent of the country and its diverse landscapes, the shift of the climatic settings is not uniformly spread (Jones et al., 2013). Although in the Zagros Mountains and also in the Taurus Mountains in Turkey forest expansion was delayed relative to the forests

in the Mediterranean (Van Zeist and Bottema, 1977; Wick et al., 2003; Stevens et al., 2006; Djamali et al., 2008; Litt et al., 2009; Schmidt et al., 2011), in both mountain sites an increase in wetness is observed since the end of the Younger Dryas. An arid steppe environment dominated by Chenopodiaceae and Artemisia is replaced by a grass steppe (Wasylikowa et al., 2006; Pickarski, 2013). Likely, the increase in wetness in the mountains was felt in the Khuzestan plain directly via an increase in precipitation as the distance between the mountain front (anticlines) and the study area is less than 100 km. An increase in wetness could also be caused indirectly via an increase in the river discharge, since all three rivers have their source in the Zagros Mountains. All above sited elements are in favour of an extension or diversification of the vegetation in the Lower Khuzestan plain. Indeed, it is observed in many cores that the vegetation was expanding at the end of the early Holocene and especially at the beginning of the mid-Holocene. The extension of a vegetation cover is most probably the result of an increase in effective wetness, possibly amplified by a rise of the groundwater table due to sea-level rise. Evidence of an increase in effective wetness during the period 8000 - 6500 yr BP is found in the central Iranian Plateau (Schmidt et al., 2011) as well as in the Mediterranean and the Levantine basin. In latter region the causes of the wetness increase are ascribed to lower mean wind speed, a higher relative air humidity, and reduced air–sea temperature differences (Rohling and De Rijk, 1999). Baeteman et al. (2004/2005) originally interpreted the vegetation on the alluvial plains as salt marshes, an interpretation that was also recalled by Heyvaert and Baeteman (2007). However, especially in arid areas typified by homogeneous clayey sediments, it remains very problematic to make a differentiation between the supratidal deposits and the (fluvial) floodplain deposits on the basis of sedimentological properties. In both environments vegetation is sparse, brackish water condition exists and the nature of the sediments -massive clayey deposits-are identical.

5.3. The nature of the widespread fluvial mud deposits

Worldwide thick fluvial mud beds are interpreted as overbank deposits. However, the combined presence of laminae or thin beds of coarser grained sediments, lags deposits, the massive structure, and the lack of interlamination in major parts of the mud deposits in combination with the huge spatial distribution of the mud, excludes solely overbank sedimentation in the study area. Therefore the mud-dominated deposits (“M1” and “M2”) most likely have also been deposited in other fluvial subenvironments. A series of studies have revealed that mud-sized particles are commonly arranged in sand-sized aggregates and are both transported and deposited within a fluvial channel (Rust and Nanson, 1989; Maroulis and Nanson, 1996; Gibling et al., 1998; Brooks, 2003; Wright and Marriott, 2007). Seasonally hot dry conditions in combination with temporary water supply give rise to cracked soils after which dry blocks disintegrate into aggregates. The more intensively the deposits are dried and the more often they are rewetted, the smaller the average aggregate diameter becomes (Vermeulen et al., 2003). The integrity of the aggregates is quickly lost due to compaction, even when the burial is shallow. The aggregate-forming mud particles consist of swelling clays, at least for a minor amount (Rust and Nanson, 1989; Maroulis and Nanson, 1996; Brooks, 2003). However, Vermeulen et al. (2003) observed the formation of aggregates also in non-swelling illite dominated clay. The mud-dominated river deposits in the Lower Khuzestan plain contain both illite and smectite, whereby illite prevails. Moreover, mud aggregates have a lower density than equally sized quartz sand and the energy level required for transporting aggregates is also lower (Maroulis and Nanson, 1996). Beside the disintegration of dry blocks, aggregates may also generate by flocculation. All favourable factors for the formation of flocs like a certain degree of salt concentration, fine-grained particles and organic material, the latter at least episodic, were part of the natural environment. The existence of both steering mechanisms make within-channel deposition quite realistic in the Lower Khuzestan plain.

6. Conclusions

A detailed study of the sediment record of the (semi)arid flat Lower Khuzestan plain allowed to document a very complex and dynamic evolution of the sedimentary environment, even in a short time interval as the last 15 000 years.

i) Although the study area is adjacent to the Persian Gulf the impact of tidal processes was restricted in time and space. The rising sea found its way inland via the existing active channels and transformed these into estuaries. No coastal or littoral zone was developed. Consequently, the transgression front had a very irregular shape rather than a smooth one. This contradicts the general image of the invading Persian Gulf as presented in publications about Mesopotamia. Also, the tidal impact lasted only 2000–2500 years.
ii) Fluvial processes predominantly modelled the landscape in the study area in the 15000 years lasting history. One regional erosional phase is registered in the record. It took place during the final phase of the Late Pleistocene. During that event several depressions were incised, separated by ridges consisting of the late Pleistocene fluvial deposits. Each depression hosted a river during the Holocene.
iii) The incision of the depressions is most probably triggered by climate. The aridification during the final phase of the Late Pleistocene in particular has played a decisive role.
iv) The sediment load of the rivers changed from predominantly sand to predominantly mud at the onset of the Holocene.
v) During the Holocene, the environment was exposed to fluctuations in the effective wetness. An increase in the effective wetness started in the early Holocene but peaked in the first half of the mid-Holocene, whereas in the second half of the mid-d the effective wetness decreased again. These fluctuations had an impact on the fluvial behaviour, the ecosystems and hydrogeochemistry.

This paper also showed that a detailed analysis of sediment characteristics can be applied successfully in terms of palaeoenvironmental evolution. This method is a useful tool and should be applied more frequently to underpin interpretations on the basis of microfossil analyses, which are often used to reconstruct former environments, especially in areas that have at first sight a uniform sedimentological up-built. Moreover, this method also provided proxies about climatic changes. Low lying areas showing hardly any relief like the Lower Khuzestan plain are generally investigated by means of coring. This paper documented the necessity that the field data should not be greatly scattered so that between-core correlations can be made, and a relative stratigraphic record be established. In this manner a comprehensive coverage in time and space can be obtained which contributes to the greater palaeoenvironmental picture.

Funding

This research was supported by the Interuniversity Attraction Poles Programme (IUAP 7/14) of the Belgian Science Policy.

Acknowledgements

The authors are very grateful to the Geological Survey of Iran, Research Institute for Earth Sciences, in particular to Razieh Lak for the logistic support during fieldwork, and to the Iran Department of Environment (Abadan Centre) for providing facilities such as guesthouse and general information. The field campaigns would not have been possible without the help of Javad Darvishi Khatoonabad and Reza Shahbazi. We thank Kim Cohen for his constructive remarks. We are also obliged to an anonymous reviewer. This paper is a contribution to the INQUA Commission on Coastal and Marine Processes.

References

Adib, A., 2008. Determination of salinity concentration in tidal rivers. J. Appl. Sci. 8, 2585–2591.
Adib, A., 2010. Extraction of structural curves, regression relations and structural regression relations in the tidal limit of the Karun River. Indian J. Sci. Technol. 3, 530–536.
Aqrawi, A.A.M., 2001. Stratigraphic signatures of climatic change during the Holocene evolution of the Tigris-Euphrates delta, lower Mesopotamia. Global and Planet. Change 28, 267–283.
Baeteman, C., Dupin, L., Heyvaert, V., 2004/2005. Geo-environmental investigation, 2. In: Gasche, H. (Ed.), The Persian Gulf Shorelines and the Karkheh, Karun, and Jarrahi Rivers: a Geo-archaeological Approach, vol. 125. Akkadica, pp. 155–215, 126(1), pp. 1–12.
Blum, M.D., Törnqvist, T.E., 2000. Fluvial responses to climate and sea-level change: a review and look forward. Sedimentology 47, 2–48.
Bogemans, F., Boudin, M., Janssens, R., Baeteman, C., 2017. New data on the sedimentary processes and timing of the initial inundation of Lower Khuzestan (SW Iran) by the Persian Gulf. The Holocene 27, 613–620.
Bronk Ramsey, C., 1995. Radiocarbon calibration and analysis of stratigraphy; the Oxcal program. Radiocarbon 37, 425–430.
Bronk Ramsey, C., 2001. Development of the radiocarbon calibration program. Radiocarbon 43 (2A), 355–363.
Brooks, G.R., 2003. Alluvial deposits of a mud-dominated stream: the red river, manitoba, Canada. Sedimentology 50, 441–458.
Dalrymple, R.W., 1992. Tidal depositional systems. In: Walker, R.G., James, N.P. (Eds.), Facies Models: Response to Sea Level Change. Geological Association of Canada, St. John's, pp. 195–218.
Dalrymple, R.W., Baker, E.K., Harris, P.T., Hughes, M., 2003. Sedimentology and stratigraphy of a tide-dominated, foreland-basin delta (Fly River, Papua New Guinea). In: Sidi, E.H., Nummedal, D., Imbert, P., Darman, H., Posamentier, H.W. (Eds.), Tropical Deltas Od Southeast Asia - Sedimentology, Stratigraphy and Petroleum Geology, vol. 76. SEPM Spec. Publ, pp. 147–173.
Day Jr., J.W., Gunn, J.D., Folan, W.J., Yáñez-Aranciba, A., Horton, B.P., 2012. The influence of enhanced Post-Glacial coastal margin productivity on the emergence of complex societies. J. Isl. Coast. Archaeol. 7, 23–52.
Djamali, M., de Beaulieu, J.-L., Shah-hosseini, M., Andrieu-Ponel, V., Ponel, Ph, Amini, A., Akhani, H., Leroy, S., Stevens, L., Lahijani, H., Brewer, S., 2008. Short Paper: a Late Pleistocene Long Pollen Record from Lake Urmia. NW Iran. https://core.ac.uk/download/files/14/336724.pdf.
Dupin, L., 2011. Mapping the landform assemblages and archaeological record of the Lower Khuzestan plain (SW Iran) using remote-sensing and GIS techniques. The Geological Society of America. Spec. Pap. 476, 53–68.
Encyclopaedia Iranica, Yarshater, E., Editor in Chief, Bibliotheca Persica Press, ISBN 1-56859-050-4, http://www.iranicaonline.org/.
Gasche, H., Paymani, A.R., 2005. Repères archéologique dans le Bas Khuzestan. In: Gasche, H. (Ed.), The Persian Gulf Shorelines and the Karkheh, Karun, and Jarrahi Rivers: a Geo-archaeological Approach, vol. 126. Akkadica, pp. 15–43, 2.
Gibling, M.R., Nanson, G.C., Maroulis, J.C., 1998. Anastomosing river sedimentation in the channel country of central Australia. Sedimentology 45, 595–619.
Hatzfeld, D., Authemayou, C., Van der Beek, P., Bellier, O., Lavé, J., Oveisi, B., Tatar, M., Tavakoli, F., Walpersdorf, A., Yamini-Fard, F., 2010. The kinematics of the Zagros mountains (Iran). In: Leturmy, P., Robin, C. (Eds.), Tectonic and Stratigraphic Evolution of Zagros and Makran during the Mesozoic-cenozoic. Geological Society, vol. 330. Special Publications, London, pp. 19–42.
Heyvaert, V.M.A., 2007. Fluvial Sedimentation, Sea-level History, and Anthropogenic Impact in the Great Mesopotamian Plain: a New Holocene Record. Unpublished PhD thesis, Brussel.
Heyvaert, V.M.A., Baeteman, C., 2007. Holocene sedimentary evolution and palaeocoastlines of the Lower Khuzestan plain (southwest Iran). Mar. Geol. 242, 83–108.
Jones, M., Djamali, M., Stevens, L., Heyvaert, V., Askari, H., Noorollahi, D., Weeks, L., 2013. Mid-Holocene environmental and climatic change in Iran. In: Petrie, C. (Ed.), Ancient Iran and its Neighbours: Local Developments and Long-range Interactions in the 4th Millennium BC. British Institute for Persian Studies and Oxbow Books, Oxford, pp. 26–35. http://e-publications.une.edu.au/1959.11/14905.
Kehl, M., Frechen, M., Skowronek, A., 2009. Nature and age of late quaternary basin fill deposits in the basin of persepolis/southern Iran. Quat. Int. 196, 57–70.
Kennett, D.J., Kennett, J.P., 2006. Early state formation in southern Mesopotamia: sea levels, shorelines, and climate change. J. Isl. Coast. Archaeol. 1, 67–99.
Kennett, D.J., Kennett, J.P., 2007. Influence of Holocene marine transgression and climate change on cultural evolution in southern Mesopotamia. In: Anderson, D.G., Maasch, K.A., Sandweiss, D.H. (Eds.), Climate Change and Cultural Dynamics: a Global Perspective on Mid-holocene Transitions. Elsevier, Amsterdam, pp. 229–263.
Knighton, D., 1984. Fluvial Forms and Processes. Edward Arnold Publishers, London.
Konyuhov, A.I., Maleki, B., 2006. Geological history, sedimentary formations, and petroleum potential. Lithol. Min. Resour. 41, 344–361.
Litt, T., Krastel, S., Sturm, M., Kipfer, R., Örcen, S., Heumann, G., Franz, S.O., Ülgen, U.B., Niessen, F., 2009. 'PALEOVAN' International continental scientific drilling program (ICDP): site survey results and perspectives. Quat. Sci. Rev. 28, 1555–1567.
Maroulis, J.C., Nanson, G.C., 1996. Bedload transport of aggregated muddy alluvium from Cooper Creek, central Australia: a flume study. Sedimentology 43, 771–790.
Masson, F., Chéry, J., Hatzfeld, D., Martinod, J., Vernant, P., Tavakoli, F., Ghafory-Ashtiani, M., 2005. Seismic versus aseismic deformation in Iran inferred from earthquakes and geodetic data. Geophys. J. Int. 160, 217–226.
Miall, A.D., 1996. The Geology of Fluvial Deposits. Springer, Berlin.
Molnar, P., 2001. Climate change, flooding in arid environments, and erosion rates. Geology 29, 1071–1074.
Molnar, P., Anderson, R.S., Kier, G., Rose, J., 2006. Relationships among probability distributions of stream discharges in floods, climate, bed load transport and river incision. J. Geophys. Res. 111 http://dx.doi.org/10.1029/2005JF000310.
Nanson, G.C., 1986. Episodes of vertical accretion and catastrophic stripping: a model of disequilibrium flood-plain development. Geol. Soc. Am. Bull. 97, 1467–1475.
NASA JPL, 2013. NASA Shuttle Radar Topography Mission Global 3 arc second number [SRTM3 data set]. Version 3. NASA EOSDIS Land Processes DAAC, USGS Earth Resources Observation and Science (EROS) Center. Sioux Falls, South Dakota. Accessed January 2015. https://lpdaac.usgs.gov. https://doi.org/10.5067/measures/srtm/srtmgl3n.003.
Pickarski, N., 2013. Vegetation and Climate History during the Last Glacial-interglacial Cycle at Lake Van, Eastern Anatolia. Universität Bonn. http://hss.ulb.uni-bonn.de/2014/3564/3564.pdf.
Pournelle, J.R., 2003. Marshland of Cities: Deltaic Landscapes and the Evolution of Civilization. Dissertation.
Reimer, P.J., Bard, E., Bayliss, A., Beck, J.W., Blackwell, P.G., Bronk Ramsey, C., Buck, C.E., Cheng, H., Edwards, R.L., Friedrich, M., Grootes, P.M., Guilderson, T.P., Haflidason, H., Hajdas, I., Hatt, Ä.C., Heaton, T.J., Hogg, A.G., Hughen, K.A., Kaiser, K.F., Kromer, B., Manning, S.W., Niu, M., Reimer, R.W., Richards, D.A., Scott, E.M., Southon, J.R., Turney, C.S.M., Van der Plicht, J., 2013. IntCal13 and MARINE13 radiocarbon age calibration curves 0-50000 years cal BP. Radiocarbon 55. http://dx.doi.org/10.2458/azu_js_rc.55.16947.
Rohling, E.J., De Rijk, S., 1999. Holocene climate optimum and Last Glacial Maximum in the Mediterranean: the marine oxygen isotope record. Mar. Geol. 153, 57–75.
Rust, B.R., Nanson, G.C., 1989. Bedload transport of mud as pedogenic aggregates in modern and ancient rivers. Sedimentology 36, 291–306.
Sanlaville, P., 1989. Considérations sur l'évolution de la Basse Mésopotamie aucours des derniers millénaires. Paléorient 15, 5–27.
Sanlaville, P., Dalongeville, R., 2005. L'évolution des espaces littoraux du golfe Persique et du golfe d'Oman depuis la phase finale de la transgression post-glaciaire. Paléorient 31, 9–26.
Schmidt, A., Quigley, M., Fattahi, M., Azizi, G., Maghsoudi, M., Fazeli, H., 2011. Holocene settlement shifts and palaeoenvironments on the Central Iranian Plateau: investigating linked systems. The Holocene 21, 583–595.
Setudehnia, A., O'B Perry, J.T., 1966. Geological Maps Marun 20830 W and Haft Kel 20830 E, Scale 1/100 000. Iranian Oil Operating Companies, Geological and Exploration Division Teheran.
Stevens, L.R., Ito, E., Schwalb, A., Wright Jr., H.E., 2006. Timing of atmospheric precipitation in the Zagros Mountains inferred from a multi-proxy record from Lake Mirabad, Iran. Quat. Res. 66, 494–500.
Sharland, P.R., Archer, R., Casey, R.B., 2001. Arabian Plate Sequence Stratigraphy, Bahrain. GeoArabia Special Publication 2, Gulf PetroLink, p. 371.
United Kingdom Hydrographic Office, 2005. Admiralty Tide Tables, 3, Indian Ocean and South China Sea. UKHO Taunton, Somerset, UK.
Van Zeist, W., Bottema, S., 1977. Palynological investigations in western Iran. Palaeohistoria 19, 19–85.
Verkinderen, P., 2009. Tigris, Euphrates, Karun, Karhe, Jarrahi. Tracking the Traces of Rivers in Lower Iraq and Khuzestan in the Early Islamic Period. Ph.D. thesis University of Gent, Belgium.
Vermeulen, J., Grotenhuis, T., Joziasse, J., Rulkens, W., 2003. Ripening of clayey dredged sediments during temporary upland disposal. J. Soils Sediments 3, 49–59.
Walker, M.J.C., Berkelhammer, M., Björck, S., Cwynar, L.C., Fisher, D.A., Long, A.J., Lowe, J., Newnham, R.M., Rasmussen, S.O., Weiss, H., 2012. Formal subdivision of the Holocene series/epoch: a discussion paper by a working group of INTIMATE (integration of ice-core, marine and terrestrial records) and the subcommission on quaternary stratigraphy (international commission on stratigraphy). J. Quat. Sci. 27, 649–659.
Walstra, J., Verkinderen, P., Heyvaert, V.M.A., 2010a. Reconstructing landscape

evolution in the Lower Khuzestan plain (SW Iran): integrating imagery, historical and sedimentary archives. In: Cowley, D.C., Standring, R.A., Abicht, M.J. (Eds.), Landscapes through the Lens: Aerial Photographs and Historic Environment. Oxbow Books, pp. 111–128.

Walstra, J., Heyvaert, V.M.A., Verkinderen, P., 2010b. Assessing human impact on alluvial fan development: a multidisciplinary case-study from Lower Khuzestan (SW Iran). Geodin. Acta 23, 267–285.

Wasylikowa, K., Witkowski, A., Walanus, A., Hutorowicz, A., Alexandrowicz, S.W., Langer, J.J., 2006. Palaeolimnology of lake zeribar, Iran, and its climatic implications. Quat. Res. 66, 477–493.

Wick, L., Lemcke, G., Sturm, M., 2003. Evidence of Lateglacial and Holocene climate change and human impact in eastern Anatolia: high-resolution pollen, charcoal, isotopic and geochemical records from the laminated sediments of Lake Van, Turkey. The Holocene 13, 665–675.

Woodbridge, K.P., Parsons, D.R., Heyvaert, V.M.A., Walstra, J., Frostick, L.E., 2015. Characteristics of direct human impacts on the rivers Karun and Dez in lowland south-west Iran and their interactions with earth surface movements. Quat. Int. 392, 315–334.

Wright, V.P., Marriott, S.B., 2007. The danger of taking mud for granted: lessons from Lower Old Red Sandstone dryland river systems of South Wales. Sediment. Geol. 195, 91–100.